



TALLINN UNIVERSITY OF TECHNOLOGY
TARTU COLLEGE

Department of sustainable technology

HYBRID NANOMATERIALS BASED ON CARBON
NANOTUBES AND METAL OXIDE NANOPARTICLES FOR
ENERGY HARVESTING APPLICATIONS

SÜSINIKNANOTORUDEL JA METALLOKSIID NANOOSAKESTEL PÕHINEVAD
NANOHÜBRIIDMATERJALID VALGUS ENERGIA KOGUMISE RAKENDAMISEKS

Master thesis
Environmental engineering

Undergraduate: Andres Aasna
Supervisor: Prof. Erwan Rauwel
Co-supervisor: Dr. Protima Rauwel

Tartu 2016

Hereby I declare that this master thesis is my original investigation and achievement.
All used materials of other authors, important statements from literature or somewhere
else originated data in this thesis are referred.

..... (signature of the author, date)

Code: 061500EAKI

Master thesis corresponds to the requirements

..... (signature of the supervisors, date)

..... (signature of the supervisors, date)

Allowed to the defence: (date)

Chairperson of the defence committee: (date)

ABSTRACT

Käesoleva uurimusliku teadustöö, mille pealkiri on „Süsiniknanotorudel ja metalloksiid nanoosakestel põhinevad nanohübriidmaterjalid valgusenergia kogumise rakendamiseks“, autor on Andres Aasna ning selle alusel taotletakse tehnikateaduste magistrikaadi. Uurimustöö on kirjutatud aastal 2016 Tallinna Tehnikaülikooli Tartu Kolledžis. Töö koosneb kahest köitest, 45 leheküljest, 4 tabelist, 19 joonisest/pildistja 50 viitest. Töö on kirjutatud inglise keeles.

Töö eesmärkideks oli täiustada hr. M. Salumaa poolt eelmisel aastal valmistatud süsiniknanotorude (CNT) ja hafniumdioksiidi nanohübriidmaterjali fotoelektrilisi omadusi lisades tsinkoksiidi (ZnO) nanoosakesi. Lisaks oli oluline eesmärk saada võimalikult palju uut informatsiooni loodud nanohübriidmaterjali omaduste kohta. Püstitatud eesmärkide täitmiseks viidi läbi järgmised toimingud:

1. Viidi läbi põhjalik kirjanduse uurimine tsinkoksiidi nanoosakestest, hafniumdioksiidi nanoosakestest ja süsiniknanotorudest.
2. Koostati kirjanduse ülevaade punktis 1 nimetatud materjalide kohta.
3. Sünteesiti tsinkoksiidi nanoosakesed nii segatuna süsiniknanotorukestega kui ka segamata.
4. Valmistati süsiniknanotoru – tsinkoksiid – hafniumdioksiid nanohübriid materjal ultrahelitöötuse teel.
5. Valmistatud nanohübriidmaterjali uuriti transmissioon-elektronmikroskoobiga (TEM).
6. Uuriti ja iseloomustati ultraheli mõju tsinkoksiidi ja hafniumdioksiidi nanoosakeste hajususele ja aglomeratsioonile etanoolis.
7. Uuriti ja iseloomustati ultraheli tekitatud kahjustusi süsiniknanotorudele.
8. Viidi läbi elektrilised mõõtmised iseloomustamiseks valmistatud materjali elektrilisi ja fotoelektrilisi omadusi.

Käesoleva töö esimene pool sisaldab kirjanduse ülevaadet tsinkoksiidi nanoosakestest, hafniumdioksiidi nanoosakestest ja süsiniknanotorudest. Välja on toodud eelnimetatud nanoosakeste olulised omadused ja sünteesimise meetodid.

Töö teine pool koosneb metoodika kirjeldusest, kasutatud materjalide ja uurimismeetodite kirjeldusest. Sellele järgneb eksperimentide kirjeldus, läbiviimise kord, tulemused ja arutelu.

Töö esimese etapina sünteesiti tsinkoksiidi nanoosakesed nii puhtal kujul kui ka segatuna süsiniknanotorudega. Prof. Erwan. Rauweli juhendamisel sünteesis uurimistöö autor neli tsinkoksiidi proovi. Selleks kasutati 20 ml tsinkatsetaati, 425 mg bensüülamiini ja kahel juhul ~6 mg mitmeseinalisi süsiniknanotorukesti. Segati 75 °C juures 15 minutit magneti abil. Tsinknanoosakesed sünteesiti mittevahelahuselise sool–geel meetodil. Selleks asetati saadud segu autoklaavi ja pandi 300 °C ahju kaheks päevaks. Segu puhastati kasutades tsentrifuugi ning seejärel kuivatati 65 °C juures.

Töö teises etapis valmistati nanohübriidmaterjal kasutades ultrahelitöötuse meetodit. Tsinkoksiidi nanoosakesed segati eelmisel aastal hr. M. Salumaa poolt valmistatud nanohübriidmaterjaliga. Kahel juhul kasutati 3 ml nanohübriidmaterjali ja 4,8 mg tsinknanoosakesi ja kahel juhul kasutati 4 mg tsinknanoosakesi segatuna süsiniknanotorudega. Uue hübriidmaterjali uurimisel kõrge resolutsiooniga transmissioon-elektronmikroskoobiga järeldati, et ultraheli on tõhus vahend osakeste hea hajususe ja kinnitumise saavutamiseks lahuses. Lisaks kinnitati eelmisel aastal saadud tulemust, et ultraheli kestvusel on otsene mõju materjalide hajususele ja osakeste kinnitumisele – pikemat aega töödeldud materjali proovid näitasid ühtlasemat hajusust ja rohkem kinnitunud osakesi. See tõdemus kehtis ka lisatud tsinkoksiidi nanosakeste kohta.

Töö autor osales Eesti ja Prantsusmaa vahelises koostööprogrammis „G. – F. Parrot“, mille eesmärk on noorteadlaste kaasamine materjaliteaduse, nanotehnoloogia, robotika, IT ja keskkonnateaduse teadusuuringutes. Sellest tulenevalt toimusid nanohübriidmaterjali elektriliste omaduste selgitamise katsed Prantsusmaal Grenobles Minatec LAHC laboris. Kohapealne juhendaja oli Dr. Frederique Ducroquet. Tulemused näitasid, et tsingi nanoosakeste lisamine materjalile muudab selle materjali elektrijuhtivust halvemaks. Elektrijuhtivuse katsed kinnitasid tsinginanosakeste isoleerivat toimet.

Kuna antud projekti raames tuli kinnitada eelmise aasta tulemusi, siis tõendati, et hr. M. Salumaa valmistatud materjalil on fotoelektrilised omadused, mis väljenduvad UV kiirguse toimel tekkivas elektrivoolus. Materjal näitas ka elektrimahtuvust, mis kutsuti esile samuti nii UV- kui ka halogeenlambi kiirgusega.

Läbiviidud katsete tulemustest saab järeldada, et ultraheli on tõhus ja lihtne viis ülal mainitud hübriidmaterjali valmistamiseks. Samuti saab väita seda, et kõnealune nanohübriid materjal on fotoelektriliste omadustega. Siiski on vajalik veelgi põhjalikum teadustöö, et materjali valmistamise protsessi täiustada ja saavutada võimalikult efektiivne nanomaterjal.

Märksõnad: metalloksiidnanoosakesed, süsiniknanotorud, nanohübriid, mitte-vesilahuseline sool – geel meetod, ultraheli, fotogalvaanika, TEM, XRD.

TABLE OF CONTENTS

ABSTRACT	3
TABLE OF CONTENTS	6
ACRONYMS AND ABBREVIATIONS	8
1. INTRODUCTION	9
1.1 History of nanotechnology	9
1.2 Nanoparticles	10
2. Literature overview of ZnO, HfO ₂ and MWCNTs	11
2.1 Nanoparticles production methods	11
2.1.2 Hydrothermal synthesis.....	11
2.1.3 Non – aqueous sol – gel	12
2.2 ZnO nanoparticles.....	12
2.2.1 History of ZnO nanoparticles	12
2.2.2 ZnO NPs properties	13
2.3 HfO ₂ nanoparticles	13
2.3.1 Discovery of HfO ₂ nanoparticles	13
2.3.2 HfO ₂ NPs properties.....	14
2.4 Multi-wall carbon nanotubes	14
2.4.1 Discovery and properties of MWCNTs	14
2.4.2 Carbon nanotubes synthesis methods.....	14
3. THE OBJECTIVES AND METHODOLOGY	15
4. EXPERIMENTAL.....	16
4.1 Introduction to TEM.....	16
4.2 Synthesis of ZnO nanoparticles and preparation of carbon-based nanohybrids	17
4.2.1 Synthesis of ZnO nanoparticles:	17
4.2.2 X-ray diffraction, XRD	17
4.2.3 HRTEM.....	19
4.2.4 Synthesis of HfO ₂ nanoparticles:	19

4.2.5	Synthesis of nanohybrid material	21
4.2.6	Electrical measurements	22
4.2.7	Sample preparation for conductivity and photocurrent measurements	22
4.2.8	Apparatus and methods	24
5.	RESULTS	25
5.1	Structural Characterization using XRD and TEM.....	25
5.1.1	XRD characterization	25
5.1.2	HRTEM characterizations.....	27
5.1.3	TEM image description of samples NANO1 to NANO4.....	29
5.2	Electrical measurements	32
6.	DISCUSSION	37
6.1	TEM studies of ZnO NPs, MWCNT–ZnO NPs	37
6.2	TEM studies of MWCNT – ZnO – HfO ₂ , effects of sonication.....	37
6.3	Electrical measurements	37
7.	SUMMARY AND CONCLUSION	39
	ACKNOWLEDGEMENTS	41
	REFERENCES.....	42

ACRONYMS AND ABBREVIATIONS

1.	Å	Angstrom
2.	Atm	Atmosphere
3.	CCVD	Catalytic carbon vapor deposition
4.	CNT	Carbon nanotube
5.	C	Celsius
6.	dV	Differential voltage
7.	HfO ₂	Hafnium dioxide
8.	HRTEM	High resolution transmission electron microscope
9.	IV	Current – voltage
10.	kV	Kilovolt
11.	MPa	MegaPascal
12.	MWCNT	Multi-walled carbon nanotube
13.	mA	Milli Ampere
14.	mV	Milli Volt
15.	NP	Nanoparticle
16.	SWCNT	Single-walled carbon nanotube
17.	SEM	Scanning electron microscope
18.	TEM	Transmission electron microscope
19.	TGA	Thermogravimetric analysis
20.	TPa	TeraPascal
21.	UV	Ultra-Violet
22.	XRD	X-ray diffraction
23.	ZnO	Zinc oxide

1. INTRODUCTION

1.1 History of nanotechnology

Along with evolution comes the need to constantly develop in all areas. Most important changes in history were partly caused by scientific discoveries. In the 4th century, craftsmen started using very small particles (nanoparticles) to change the properties of materials. Irrespective of their theoretical background, they worked with empirical acknowledgement and manipulation of materials. The Lycurgus Cup (Rome) is an example of dichroic glass where colloidal gold and silver in the glass makes it opaque green when lit from outside but translucent red when light shines through the inside [1]. These empirical acknowledgements passed on from generation to generation. Between the 6th to 15th centuries, European cathedrals were decorated with vibrant stained glass windows consisting of nanoparticles of gold chloride and other metal oxides and chlorides. Between the 13th and 18th centuries people started using carbon nanotubes and cementite nanowires to create “Damascus” sword blades [2].

Even though nanoparticles had been already used for centuries, it was not until 1974 that N. Taniguchi at a conference, provided a definition for it [3]. He defined nanotechnology as mainly consisting of the processing of separation, consolidation, and deformation of materials by one atom or one molecule. But before Norio Taniguchi’s speech in 1974, Richard P. Feynman in 1959 gave his first lecture on technology and engineering at the atomic scale, “There is Plenty of Room at the Bottom” [4]. In the 1980s, one of the nanotechnology developers K. Eric Drexler published a book called “Engines of Creation” [5], where he discusses the effects of the technological achievements and gives very ambitious but well-reasoned examples. In the same year (1986) when Drexler published his book, atomic force microscopy was also invented, which had the capability to view, measure and manipulate materials down to fractions of a nanometre. It was not until the early nineties that nanotechnology companies like Nanophase Technologies, Helix Energy Solutions Group came into the spotlight [1]. Also with TEM analysis coming into the forefront, nanotechnology was given a boost as it was actually possible to visualize these nanostructures. This was the decade when many new properties of nanoparticle were discovered including their structure and their synthesis was further developed. Along with the rising demand for better materials came the need to form working groups to make an

inventory of the state of art at the nanoscale and set forth possible future developments. In 1998 The Interagency Working Group on Nanotechnology (IWGN) was created leading to the formation of the U. S. National Nanotechnology Initiative in (NNI) 2000 [6]. The beginning of the 21st century was nevertheless the starting point for the use of nanotechnology to make consumer products like car bumpers or even golf balls.

During the last 16 years there has been a lot of research aimed at using nanotechnology in order to solve two of the biggest problems in the world. First is the need to produce more efficient and cheaper medical applications, second is the need to find solutions to the ongoing energy crises. Governments in different countries are therefore funding scientific research in the field of nanotechnology. USA congress funded the NNI for the first time in 2001 [1]. In 2004 SUNY Albany launched the first college-level education program in nanotechnology in the United States, The College of Nanoscale Science and Engineering [7]. The universities all over the world are making efforts towards working out new and better solutions for our problems. Even small countries like Estonia contribute to the development of nanotechnology. This includes Estonian Nanotechnology Competence Centre project [8]. Also Estonian universities are working closely with foreign universities in the same aim. Some part of this Masters' thesis has benefitted from a Franco-Estonian cooperation program called the Parrot program.

1.2 Nanoparticles

Nanoscale has been defined to denote the size approximately from 1 nm to 100 nm [9]. The prefix nano- is also used in SI units to indicate 10^{-9} m. Nano-objects can have different shapes. Most common are nanoparticles (3 external dimensions in the nanoscale), nanofibres (2 external dimensions in the nanoscale) and nanoplates (1 external dimensions in the nanoscale) [9]. In this master thesis there are three main nano-objects: ZnO and HfO₂ nanoparticles combined with multi-walled carbon nanotubes (MWCNT-s). These compounds will be described in the next paragraph.

2. Literature overview of ZnO, HfO₂ and MWCNTs

Nanotechnology is one of the fastest developing branches of science due to its wide range of applications. According to the literature the usage of nanoparticles extends from the food industry to energy production [10, 11]. The nanoparticles have proven to make materials and applications so much better in quality and efficiency. Scientific research work on NPs has been growing rapidly since the early nineties. One of the most studied is carbon nanotubes due to its outstanding mechanical and electrical properties. Over the last 25 years the research was mainly about different nanoparticles separately but the current thesis is focused on studying a nanohybrid composite of CNTs mixed with ZnO and HfO₂ nanoparticles for possible energy harvesting applications.

2.1 Nanoparticles production methods

Metal oxide nanoparticles syntheses methods can generally be split into two: ‘bottom-up’ and ‘top-down’. The former means that preparation starts from atomic or molecular precursors, which come together to form clusters. „Top-down” is a process when nanoscale is reached by physically making the larger particles smaller [12]. The following section is overview of the different methods of synthesizing metal oxide nanoparticles and carbon nanotubes.

2.1.1 Mechanical

Ball milling is a top-down synthesis technique where the bulk materials size is reduced mechanically by crushing. This method is used also in industry for producing fine powders like cement and clay. It also has found great acceptability especially in industrial nanomaterial preparation environments due to the simplicity, versatility of the process (can be adapted to make many types of nanomaterials) and cost-effective scalability of the process [13]. One of the major disadvantages is that the size of particles produced is uncontrollable and irregular [14].

2.1.2 Hydrothermal synthesis

Hydrothermal synthesis is a method used to produce metal oxide crystals from metal salt aqueous solutions by heating the aqueous solution [15]. Generally defined as crystal synthesis

or crystal growth under high temperature and high pressure water conditions from substances which are insoluble in ordinary temperature and pressure (100°C, 1atm) [16]. The hydrothermal synthesis method is typically used with a batch type autoclave, where aqueous solution is heated up slowly up to 100 – 300°C and then aged for several hours or days [17]. The particle size of metal oxide depends on the hydrolysis rate and solubility of the metal oxide. Hydrothermal synthesis in supercritical water has advantages for synthesis of multi metal oxide compounds because the reaction rate is enhanced more than 10^3 times that under the conventional hydrothermal conditions [18 - 20].

2.1.3 Non – aqueous sol – gel

In non-aqueous sol-gel chemistry the transformation of the precursor takes place in an organic solvent under exclusion of water. The list of potential precursors includes inorganic metal salts, metal alkoxides, metal acetates and metal acetylacetonates. The oxygen for nanoparticle formation is provided by the solvent (ethers, alcohols, ketones, or aldehydes) or by the organic constituent of the precursor (alkoxides or acetylacetonates) [21]. Non-aqueous processes can roughly be divided into surfactant- and solventcontrolled approaches. In the first case typical temperature range is around 250 to 350°C and for the solventcontrolled approach the temperature is little lower ~ 50 to 200°C [22].

Advantages of non-aqueous sol-gel chemistry is that the control over particle sizes, shapes and compositions is possible because of the large variety of organic solvents and the well understood organic reaction processes [21, 23]. One more advantage is that this method can be used for synthesizing many different metal oxide nanoparticles like ZnO, HfO₂, TiO₂, CrO, MoO₃, ZrO₂, SiO₂ [24].

2.2 ZnO nanoparticles

2.2.1 History of ZnO nanoparticles

Studies of zinc oxide carried out since 1935 as is therefore a well-known material [25]. During the last eighty years there have been a lot of different studies such as optical properties, growth by chemical-vapor transport, vibration properties and metal-insulator-

semiconductor structures. The result is that current industry relies upon ZnO, due to the development of growth technologies for the synthesis of high quality single crystals and epitaxial layers, allowing for the realization of ZnO-based electronic and optoelectronic devices. Also in many industrial manufacturing processes including paints, cosmetics, pharmaceuticals, plastics, batteries, electrical equipment, rubber, soap, textiles, floor coverings etc. With improvements in growth technology of ZnO nanostructures, epitaxial layers, single crystals and nanoparticles, ZnO devices have already become functional in everyday life.

2.2.2 ZnO NPs properties

The ZnO nanoparticles studied in this Masters work were synthesized using non-aqueous sol-gel process. This process was described above. Zinc oxide is classified as a semiconductor in group II-VI, whose covalence is on the boundary between ionic and covalent semiconductors. ZnO crystallizes in blend or hexagonal wurtzite structure and has direct band gap of 3.37 eV at ambient conditions. Compared to other metal oxides has ZnO relatively high and stable exciton binding energy of 60 meV at room temperature [26, 45]. ZnO nanoparticles emit light both in visible and UV range of spectrum. Due to these specific properties ZnO has high potential in many applications such as photovoltaic [27], optical [28], magnetic [29], and electronic [30] devices also in medicine [31].

2.3 HfO₂ nanoparticles

2.3.1 Discovery of HfO₂ nanoparticles

Hafnium dioxide bulk material has been known already for almost 85 years [32]. Only in the last 20 years, it has been researched more closely. Hafnium dioxide is a dielectric material with properties that mainly appeal to micro/nano-electronic devices. In an effort to make chips smaller and faster, HfO₂ can be used instead of traditional silicon dioxide because hafnium dioxide has a high dielectric constant.

2.3.2 HfO₂ NPs properties

As mentioned above hafnium dioxide has excellent properties for applications in the fields of electronics due to its high dielectric constant ($k > 25$) and wide band gap ($E_g \sim 5,7$ eV) [33]. The hafnium dioxide nanoparticles used in this study are moreover luminescent due to their surface states. This makes it a good candidate for optoelectronic applications.

2.4 Multi-wall carbon nanotubes

2.4.1 Discovery and properties of MWCNTs

Since 1991, when the carbon nanotubes were discovered, there has been increasing interest in this material. Today, the CNTs have become one of the most studied materials. CNTs have unique electronic, mechanical, catalytic, adsorption, and transport properties, making them useful for a variety of applications. There are two main types of CNTs: single-wall (SWCNT) and multi-wall carbon nanotubes (MWCNT). In this Masters work, we use MWCNT because they exhibit excellent electrical conductivity. This phenomenon is caused by chirality which means the direction in which graphene sheets are rolled into tubes [34].

2.4.2 Carbon nanotubes synthesis methods

The oldest method for the carbon nanotube production is the electric arc discharge. There are also solar technique, electrolysis, hydrothermal synthesis, chemical vapour deposition method and laser ablation method [35]. In this research article, the advantages and disadvantages of different CNT synthesis methods are clearly described. Based on this article the best production method for large scale production of MWCNTs is chemical vapour deposition method.

3. THE OBJECTIVES AND METHODOLOGY

The objective of the current thesis is to confirm the results of research work done by Mr. Martin Salumaa last year and also to study electrical and photocurrent properties of ZnO-HfO₂-CNT nanohybrid material. This Masters' thesis was initiated by Prof. Erwan Rauwel and Dr. Protima Rauwel from University of Tartu. The aim was to confirm whether the photocurrent observed last year with HfO₂ mixed MWCNTs under UV and visible light excitation was reproducible. The production of photocurrent in case of ZnO mixed with MWCNTs was also checked. The plan was to study the influence of ZnO nanoparticles to the optimize parameters. This research project was carried out in collaboration with Minattec LAHC in Grenoble France via a PARROT project between Estonia and France. This collaboration included experiments to investigate the electrical-photogalvanic properties. These studies were carried out in collaboration with Dr. Frederique Ducroquet. The outcomes of these experiments will be presented in results and discussion section.

To achieve the objectives, methodology consists of the following tasks:

1. Synthesis of ZnO nanoparticles
2. Research of metal oxide nanoparticles and CNTs
3. Synthesis of the MWCNTs –ZnO –HfO₂ hybrid nanocomposites via sonication
4. TEM studies of the synthesized hybrid nanocomposites.
5. Sonication effects on the dispersion and agglomeration of ZnO and HfO₂ NPs
6. Defects in CNTs induced by sonication
7. Electrical and photocurrent measurements of samples synthesized at different sonication times samples

4. EXPERIMENTAL

4.1 Introduction to TEM

A transmission electron microscope involves a high voltage electron beam (usually ~200kV). In fact, electrons are emitted by a cathode and focused by electromagnetic lenses to form a beam. The electron beam that has been transmitted through a very thin (20- 500 nm) specimen carries information about the structure of the specimen. The spatial variation in this information (the "image") is then magnified by a series of magnetic lenses until it is recorded by hitting a fluorescent screen, photographic plate, or light sensitive sensor such as a CCD (charge-coupled device) camera. The image detected by the CCD may be displayed in real time on a monitor or computer [36, 38].

In order to understand the material properties we need to have TEM images which then help us correlate them to the structure of the material. The images can be used to determine the crystal structure of a material and features like dislocations and grain boundaries. Chemical analysis can also be performed. TEM can be also used to study the nature of the growth of layers as in thin films, their composition and defects in semiconductors. High resolution can be used to analyse the quality, shape, size and density of quantum wells, wires and dots with atomic size precision [37]. For carbon nanomaterials, TEM is the only tool that can study the morphology (i.e. nanostructure) of the material and can study defects in the carbon based structures [38]. TEM can be used to distinguish between a carbon nanotube and a carbon nanofiber; which otherwise may look similar when observed by scanning electron microscope (SEM).

Based on the literature ZnO has been one of the most investigated materials during the last two decades. For ZnO, TEM has been systematically used for studying the material at the nanoscale. For example co-workers have been using TEM to characterize CuO and ZnO nanostructures grown under different durations of synthesis [39]. There are many more scientific articles, thesis and research papers where TEM is used to characterize and analyse the studied materials [40, 41].

In this Masters' thesis the TEM images were used to analyse the synthesized samples. Since these materials are used for energy harvesting applications, the nature of the bonding between

nanoparticles and CNTs has to be studied. This implies that a more efficient energy transfer from the nanoparticles to the nanotubes is possible if the ZnO and HfO₂ nanoparticles are in contact with the CNTs. Checking the decoration of the nanoparticles at the nanoscale is only possible via TEM. Here, we are also able to understand the effect of the temperature of synthesis on the size and morphology of the nanoparticles. The information from the images is essential for understanding and comparing the samples to each other.

4.2 Synthesis of ZnO nanoparticles and preparation of carbon-based nanohybrids

4.2.1 Synthesis of ZnO nanoparticles:

The procedure for synthesizing ZnO nanoparticles was carried out under air. In a typical synthesis, Zinc acetate (2.73 mmol) (99.99%, Aldrich) was added to 20ml (183mmol) benzylamine (Aldrich). The reaction mixture was transferred into a stainless steel autoclave and carefully sealed. Thereafter, the autoclave was heated in a furnace at a temperature of 200°C, 240°C or 300°C for 2 days. The resulting milky suspensions were centrifuged, the precipitates thoroughly washed with ethanol and dichloromethane and subsequently dried in air at 60°C.

4.2.2 X-ray diffraction, XRD

X-ray diffraction (XRD) was first proposed by Sir W. H. Bragg and his son Sir W. L. Bragg in 1913 [46]. It is a powerful technique for characterizing crystalline materials structures, phases, and other structural parameters, such as average grain size, crystallinity, strain, and crystal defects. X-ray diffraction peaks are produced by constructive interference of a monochromatic beam of x-rays scattered at specific angles from each set of lattice planes in a sample [42]. These diffraction patterns give an indication of the general structure of the sample. The explanation of Bragg condition is given in the following section.

X-Ray diffraction also known as Braggs law can be derived by considering the conditions necessary to make the phases of the beams coincide when the incident angle (θ) and reflecting angle (θ) are equal (Figure 1). The second incident beam b continues to the next layer where it is scattered with the next layers of atom C. Beam b must travel the extra distance BC + CD if

the two beams a and b are to continue travelling adjacent and parallel. This extra distance must be an integral (n) multiple of the wavelength (λ) for the phases of the two beams to be the same [46, 47].

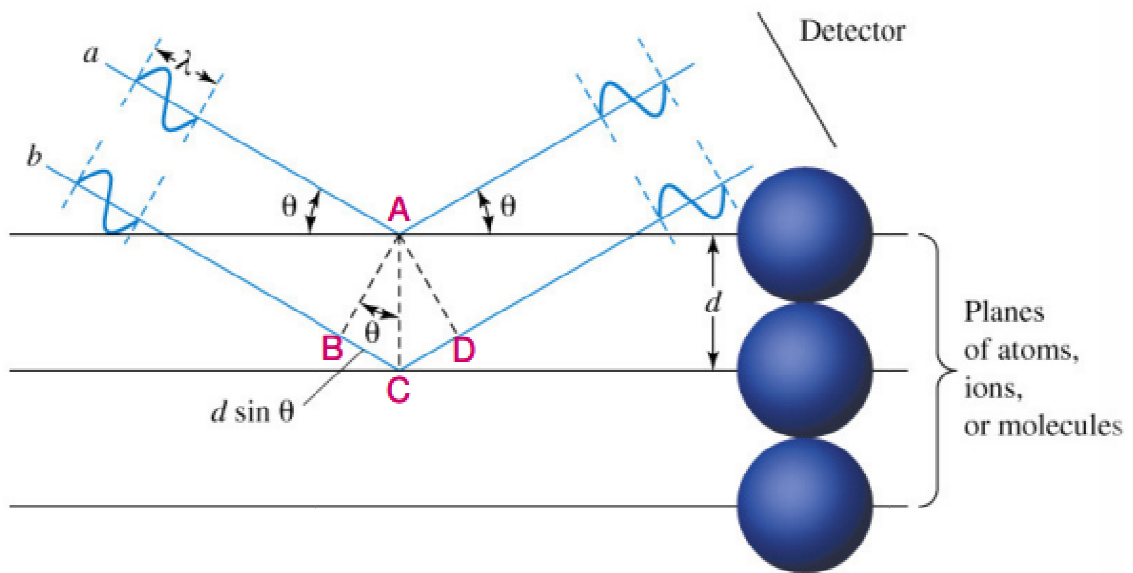


Figure 1. Derivation of Bragg's Law [47].

The distance B to C is the same as C to D and $BC = d \cdot \sin\theta$ then the Bragg's Law is [46]:

$$n \cdot \lambda = 2 \cdot d \cdot \sin\theta \quad (\text{Eq. 1})$$

where

- λ – wavelength of the characteristic X-ray (nm)
- d – latticeinterplanar spacing of the crystal (nm)
- θ – X-ray incidence angle (Bragg angle) (degrees)
- n – number of the wavelength which beam b is behind beam a (value)

XRD patterns were obtained using Bruker D5000 XRD instrument equipped with a Braun position sensitive detector, both using Cu K_{α} radiation.

In order to estimate the size of the nanoparticles it is possible to use several methods. These methods are the Scherrer, the Williamson-Hall, the Warren-Averbach, but it is also possible to

combine these methods [49]. In this Masters' thesis we have applied the Scherrer equation (2) [48, 50]:

$$T = \frac{K\alpha*\lambda}{\beta*cos\theta} \quad (\text{Eq. 2})$$

where

- T – average crystallite size (nm)
- λ – the K radiation (nm)
- β – the width of the peak at half of the maximum intensity (radian).
- K_{α} – constant related to crystallite shape, normally taken as 0.9
- θ – X-ray incidence angle (Bragg angle) (degrees)

The Scherrer equation is meant to calculate crystalline sizes on the nanoscale. This equation relates the size of crystallites in a solid to the broadening of a peak in a diffraction patterns. The XRD patterns are presented in Figure 4 and 5.

4.2.3 HRTEM

High resolution transmission electron microscopy (HRTEM) was carried out on a G2 80–200 FEI Titan, operating at 200 kV, disposing a point to point resolution of 0.9 Å. The point to point resolution in TEM mode is 2.4 Å. HRTEM (High Resolution Transmission Electron Microscopy) is an imaging mode of TEM for high magnification studies of nanomaterials. Although scanning electron microscopes (SEM) produce three-dimensional (3D) images while TEM only produces flat (2D) images which are projections of the sample [43], for this thesis is important to investigate nanohybrid material in high magnification and on greater resolution.

4.2.4 Synthesis of HfO₂ nanoparticles:

The procedure for synthesizing HfO₂ nanoparticles was carried out in a glove box (O₂ and H₂O < 1 ppm). In a typical synthesis, hafnium tert-butoxide (Hf(OtBu)₄) precursor (STREM 99.9%) (0.87 mmol) was added to 20 ml (183 mmol) of benzylamine (purified by redistillation (99.5%), Aldrich) for the synthesis of cubic HfO₂ nanoparticles. The reaction mixture was

transferred into a stainless steel autoclave and carefully sealed. Thereafter, the autoclave was taken out of the glove box and heated in a furnace at 300°C for 2 days. The resulting milky suspensions were centrifuged; the precipitates were thoroughly washed with ethanol and dichloromethane; and subsequently dried in air at 60°C.

Contrary to the HfO₂ nanoparticles that were synthesized at the University of Oslo in 2011, the ZnO nanoparticles used in this research work were prepared at Tartu College. In all 10 samples based on ZnO, HfO₂ and CNTs have synthesized for this work, 6 of these samples were synthesized using an autoclave at different temperatures. The 3 samples ETCZn003 to ETCZn005 are carbon based nanohybrid materials that were synthesized using ZnO precursor mixed with MWCNTs. The samples ETCZn001, ETCZn002 and ETCZn006 correspond to pure free-standing ZnO nanoparticles that were synthesized at 200°C, 240°C and 300°C, respectively. The other four samples NANOH1 to NANOH4 were produced by mixing cubic HfO₂ nanoparticles (samples ERHf001) with the previously synthesized with ZnO MWCNTs nanohybrids samples (ETCZn003, ETCZn004 and ETCZn005). The complete description of the synthesis of these 6 samples will be explained in the following sections. All the quantities, materials and temperatures are shown in Table 1.

Table 1. Samples synthesised

Samples	Temp. synth. °C	Precursor 1	Mass 1 (mg)	Precursor 2	Mass 2 (mg)	Solvent (ml)	Compound
ETCZn001	200	Zn(acetate) ₂	600			B. amine (20)	ZnO
ETCZn002	240	Zn(acetate) ₂	506			B. amine (20)	ZnO
ETCZn006	300	Zn(acetate) ₂	461			B. amine (20)	ZnO
ETCZn004	200	Zn(acetate) ₂	376	MWCNTs	4,0	B. amine (20)	ZnO_MWCNTs
ETCZn003	240	Zn(acetate) ₂	350	MWCNTs	4,5	B. amine (20)	ZnO_MWCNTs
ETCZn005	300	Zn(acetate) ₂	425	MWCNTs	6,0	B. amine (20)	ZnO_MWCNTs

The TEM images provide us important information about the synthesised hybrid nanocomposite (nanoparticle size and distribution) especially for the ZnO nanoparticles connected to MWCNTs. TEM study will highlight how the sonication time affects the bonding between the metal oxide nanoparticles (ZnO and HfO₂) and the MWCNTs. It also

should show the best condition of synthesis and how it is possible to tune the morphology of the produced hybrid nanomaterial.

4.2.5 Synthesis of nanohybrid material

This Master's thesis is the continuation of Mr. Martin Salumaas Master's thesis on "Hybrid nanomaterials based on carbon nanotubes and metal oxide nanoparticles for photovoltaic applications". Based on Mr. Salumaas electrical measurements and research work the nanohybrid materials were further studied and developed in this thesis. New samples which brought together HfO₂, ZnO nanoparticles and carbon nanotubes were synthesized here. It was decided to use for the next step samples ETCZn005 and ETCZn006 because the TEM images showed that ZnO nanoparticles synthesized at 300°C are more suitable for the purpose of this thesis. Samples ETCZn005 and ETCZn006 had good dispersion of the particles and carbon nanotubes. Table 2 given below describes all the information (quantities and sonification time).

Table 2. Quantities and sonification time

Samples	Sonification time (min)	Precursor 1	Volume 1 (ml)	Precursor 2	Mass 2 (mg)	Sonicated after 30 and 90 min for 5 min	Mass 3 (mg)
NANOH1	30	EHf001	3,0	ETC006	4,8		
NANOH2	30	EHf001	2,0			ETCZn005	4,6
NANOH3	90	EHf001	3,5	ETC006	5,3		
NANOH4	90	EHf001	2,5			ETCZn005	4,4

For this study, a previous mixture of 6 mg of MWCNTs mixed with 7.9 mg of HfO₂ cubic nanoparticles from sample ERHfO001 was used. For NANOH1 4.8 mg of ZnO nanoparticles (sample ETCZn006) were added to 2.0 ml of HfO₂/MWCNTs solution and completed with 1.0 ml of pure ethanol. The mixture was then shaken manually for 2 to 5 minutes before being transferred in an ultrasound bath for 30 minutes.

NANOH2 corresponds to 2.3 ml of HfO₂/MWCNTs previously used, but without ZnO nanoparticles, to be used as reference. This sample was also transferred in to an ultrasound bath for 30 minutes. After that ultrasonic treatment, 4.6 mg of ZnO/MWCNTs nanohybrid synthesized at 300°C were added to this sample and then transferred into the ultrasonic bath

for 5 minutes. The other two samples were synthesized using exactly the same procedure, but the ultrasound treatment time was extended to 90 minutes. Amounts of the ingredients used for the synthesis of NANO_{H3} and NANO_{H4} are shown in the table above.

4.2.6 Electrical measurements

Electrical measurements were carried out in MINATEC laboratory under the supervision of Dr. Frédérique Ducroquet. All equipment necessary for preparation of the samples was provided. Samples were prepared using different methods for getting better results for measuring photoelectrical properties.

4.2.7 Sample preparation for conductivity and photocurrent measurements

Samples were deposited on the glass support by depositing a droplet of liquid containing the hybrid nanocomposite using a pipette. When the ethanol had evaporated, the samples were visually inspected under the microscope (Figures 2 and 3). As ethanol straggled on the glass support we decided to heat the support to 75 °C for faster evaporation of ethanol. In order to obtain more information about the heating effect, all the samples were prepared using both ways (Figure 3). Table 3 gives the overview of all the prepared samples, measurements taken and the nature of the support it was used.

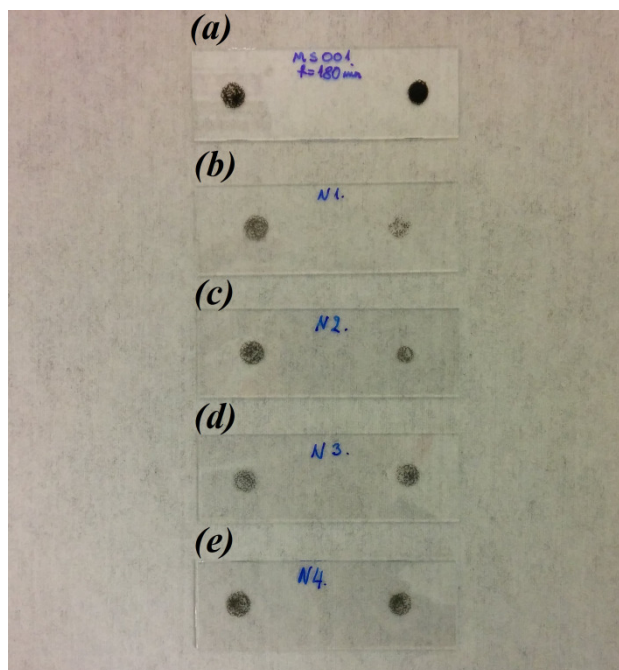


Figure 2. Samples for conductivity and photocurrent measurements (a): MS001 ($t=180$ min), (b): NANO1, (c): NANO2, (d): NANO3, (e): NANO4.

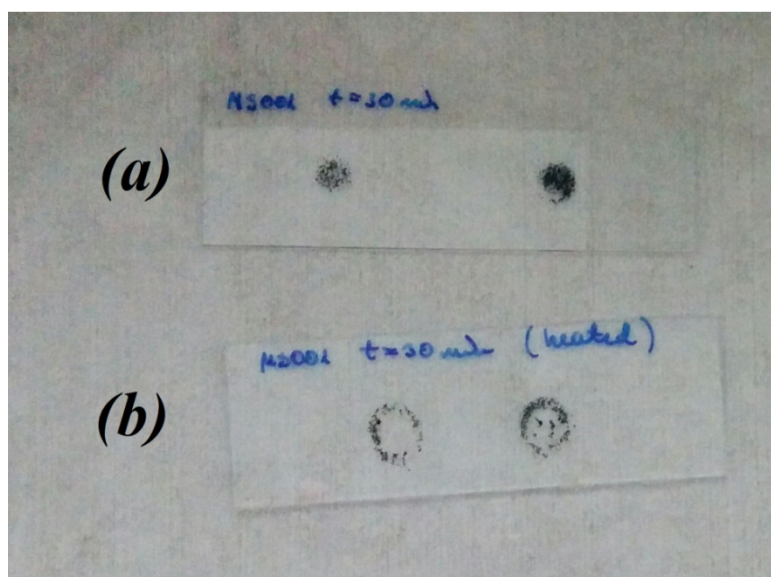


Figure 3. Samples on the heated glass support. Unheated support (a): MS001 ($t=30$ min), Support heated to $75\text{ }^{\circ}\text{C}$ (b): MS001 ($t=30$ min).

Table 3. Overview of all the prepared samples

Samples	Measurement		Support type (quantity)	
	Electrical conductivity	Photocurrent	Support on room temp. (quantity)	Support on 75 °C (quantity)
MS001 (t=180min)	x	x	3	2
MS001 (t=120min)	x	x	2	1
MS001 (t=40min)	x	x	1	2
MS001 (t=30min)	x	x	4	3
MS001 (t=20min)	x	x	2	2
MS001 (t=10min)	x	x	1	1
MS001 (t=0min)	x	x	1	1
NANO1	x	x	1	
NANO2	x	x	1	
NANO3	x	x	1	
NANO4	x	x	1	
ETCzn005	x	x	1	1
x - the measurements were performed				

4.2.8 Apparatus and methods

Photocurrent, IV, dV measurements were carried out using a Hewlett – Packard 4155A Semiconductor Parameter Analyser.

For photocurrent measurements, the samples were first tested for conductivity and IV–curves (current and voltage, respectively) were constructed, both in the dark and under illumination by halogen lamp and UV-lamp. IV–curves show conductivity through the sample and help to determine whether or not there is a contact between the contacts on the support through the material. Halogen light and UV light was used to see if they have an effect on the conductive properties of the material. Moreover, dV measurements were done to see photocurrent generation under illumination by halogen and UV.

All prepared samples were tested for conductivity and photocurrent effect. During the stay in Grenoble it was prepared 20 samples and recorded 162 measurements.

5. RESULTS

5.1 Structural Characterization using XRD and TEM

5.1.1 XRD characterization

All samples have been characterized using XRD. The XRD study has been performed in Portugal at the University of Aveiro, CICECO. All the XRD patterns show that the ZnO nanoparticles are highly crystalline. The XRD patterns on Figures 4 and 5 show that particles are highly crystalline with the hexagonal wurtzite-analogous ($P6_3mc$) crystal structure ($a = 3.25\text{\AA}$ and $c = 5.20\text{\AA}$). The addition of MWCNTs in the precursor mixture before the synthesis does not seem to affect the crystallinity of the ZnO nanoparticles.

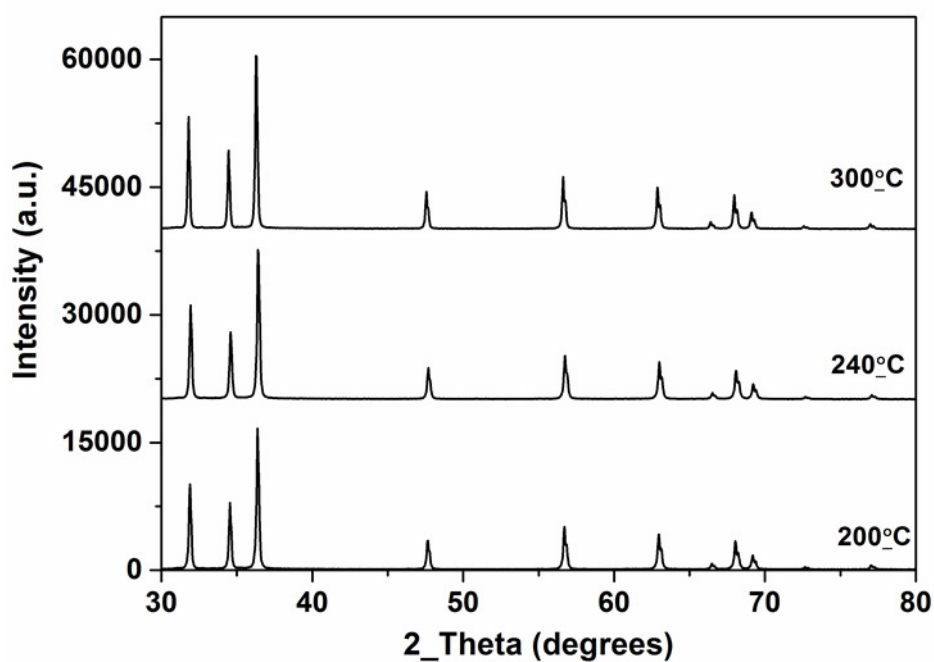


Figure 4. X-ray diffraction pattern of ZnO NPs synthesized on 200, 240 and 300 °C.

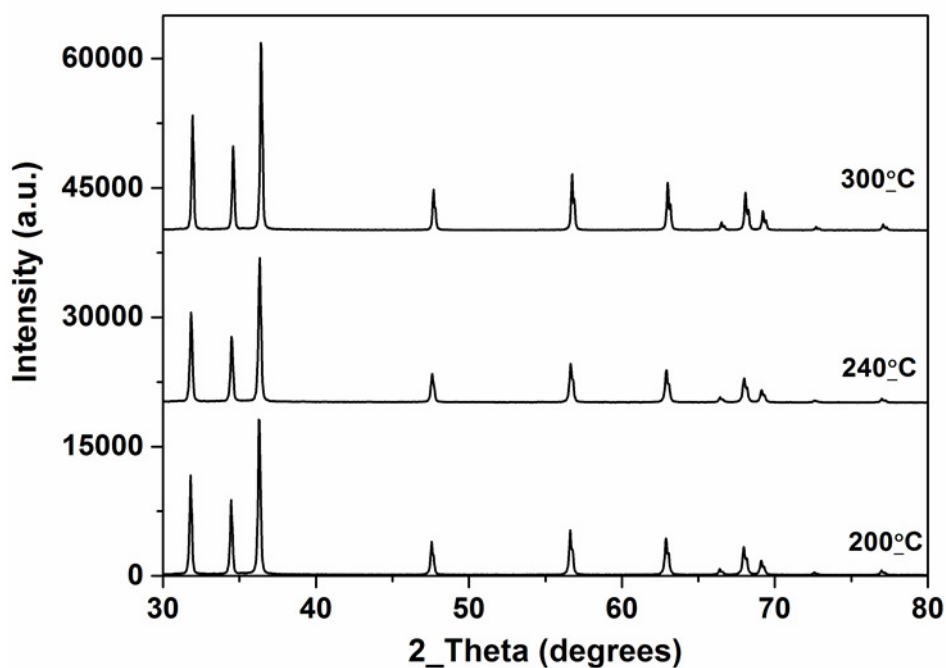


Figure 5. X-ray diffraction patter of ZnO mixed with MWCNTs NPs synthesized on 200, 240 and 300 °C.

To estimate the ZnO NP size we applied the Scherrer equation to the 6 XRD patterns. In Table 4 the size of the nanoparticles are calculated by using the equation (2). These calculations are estimation for better understanding the synthesis process and to compare to the ones obtained from TEM study.

Table 4. Estimation of the size of the ZnO nanoparticles using the Scherrer equation.

Name	Composition	Temperature (°C)	Nanocrystallites size (XRD) nm
ETCZn001	ZnO NPs	200	122
ETCZn002	ZnO NPs	240	112
ETCZn006	ZnO NPs	300	141
ETCZn004	ZnO NPs + MWCNTs	200	146
ETCZn003	ZnO NPs + MWCNTs	240	50
ETCZn005	ZnO NPs + MWCNTs	300	124

5.1.2 HRTEM characterizations

5.1.2.1 ETCZn004

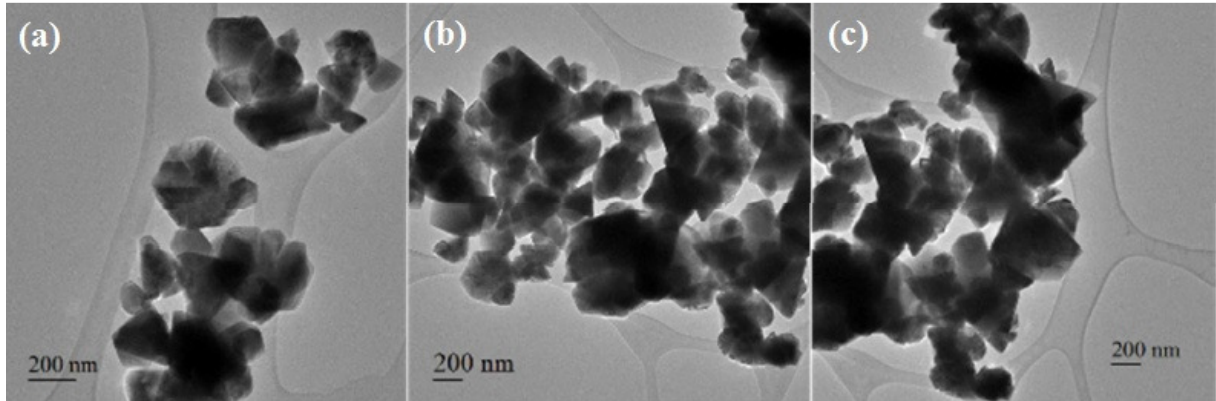


Figure 6. TEM image of sample ETCZn004.(a), (b) and (c) overview of the sample.

For the sample synthesized at 200°C TEM images are given here above. Here the 3 images illustrate that the diameter is the range of 100 to 400 nm. On image 6(a) it can be seen clearly that nanoparticles are hexagonal and triangular shape with rather sharp edges. Figure 6(b) and(c) illustrate that the nanoparticles are agglomerated.

5.1.2.2 ETCZn003

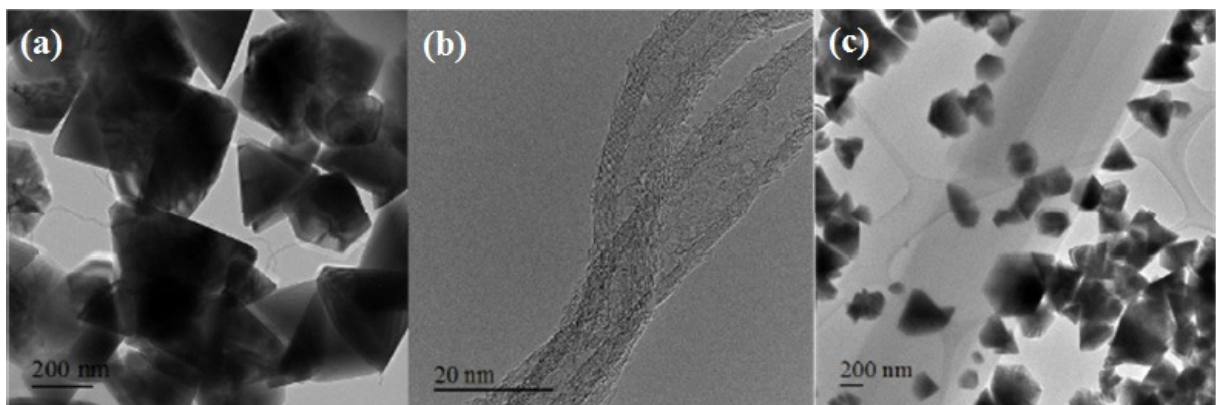


Figure 7. TEM image of sample ETCZn003. (a) and (c) give the overview of the sample, (b) HRTEM image of a MWCNT-s.

Sample ETCZn003 was synthesized at 240°C. Figure 7(a) and (c) show that ZnO NPs are agglomerated to each other and also attached to CNT. On the first image the nanoparticles

have diameter around 150 to 500 nm with triangular shape and have very sharp edges. Also in Fig. 7(a) it is noticeable that the CNTs are attached to some ZnO NPs. In Fig. 7(b) a high magnification micrograph of MWCNT illustrates that the number of walls of the MWCNTs are not the same for the 2 tubes. The two CNTs with diameters ranging from 10 to 15 nm and they have up to 10 walls. It is also visible that the CNT walls are not straight and there is an indication of amorphous carbon and these could be formed via sonication. Figure 7(c) reveals that ZnO nanoparticles have in addition to triangular shape hexagonal shaped NPs.

5.1.2.3 ETCZn005

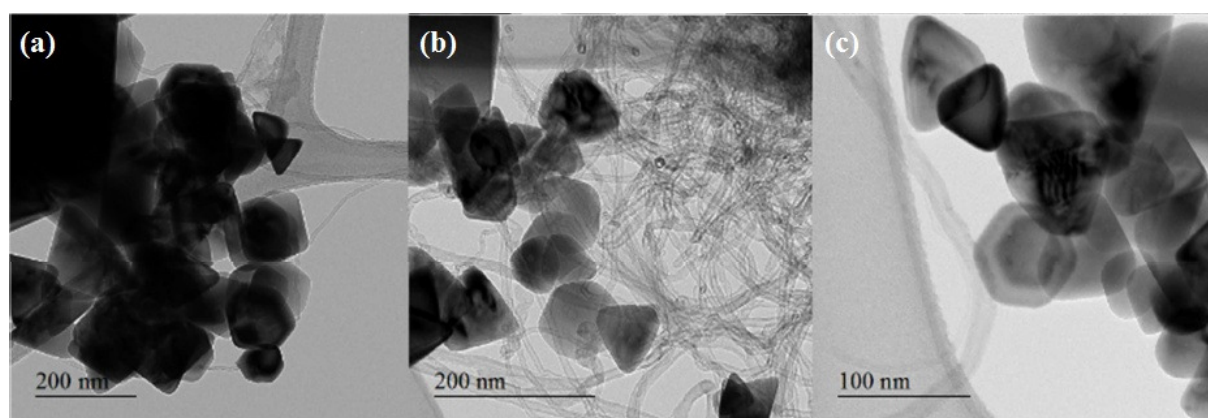


Figure 8. TEM image of sample ETCZn005. (a) and (b) give the overview of material, (c) is the magnification from the material.

This sample was synthesized in an autoclave at a temperature of 300°C. Figures 8(a) and (b) show that the ZnO nanoparticles are well contacted with CNTs. Size of ZnO NPs is around 50-100 nm with different morphologies and structure. In Figure 8(a) is clearly visible hexagonal, triangular and quadrilateral shaped NPs. The edges of ZnO nanoparticles are not so sharp compared to sample ETCZn004 and ETCZn003. Higher magnification (c) reveals that CNTs and ZnO NPs are connected to each other and CNTs have diameter around 10 to 15 nm. Compared to Figure 6(a), Figure 8(b) reveals at a higher magnification the connectivity of the nanoparticles to the nanotubes.

5.1.2.4 ETCZn006

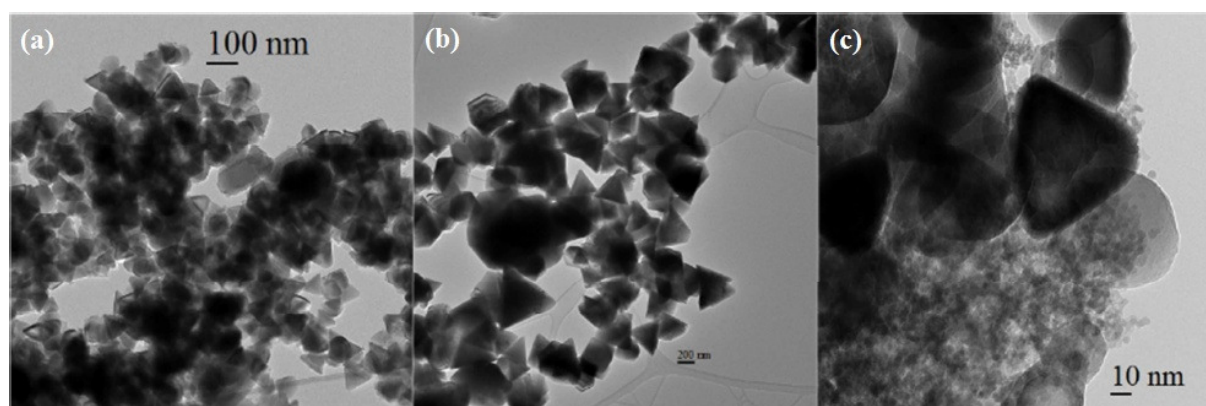


Figure 9. TEM image of sample ETCZn006. (a) and (b) overview of the material, (c) high magnification image of ZnO NPs.

ETCZn006 sample is synthesized in an autoclave around 300°C. Figure 9(a) is giving us valuable information about nanoparticle size and shape. Size of ZnO NPs is around 50 to 400 nm some of the particles have even larger diameters as in Fig. 9(b). Although the triangular shape, which corresponds to pyramidal body structure, is dominating there is also hexagonal and quadrilateral shaped NPs. Fig. 9(c) brings out very clearly that there are smaller ZnO particles with diameter of 30 and even smaller.

5.1.3 TEM image description of samples NANOH1 to NANOH4

5.1.3.1 NANOH1

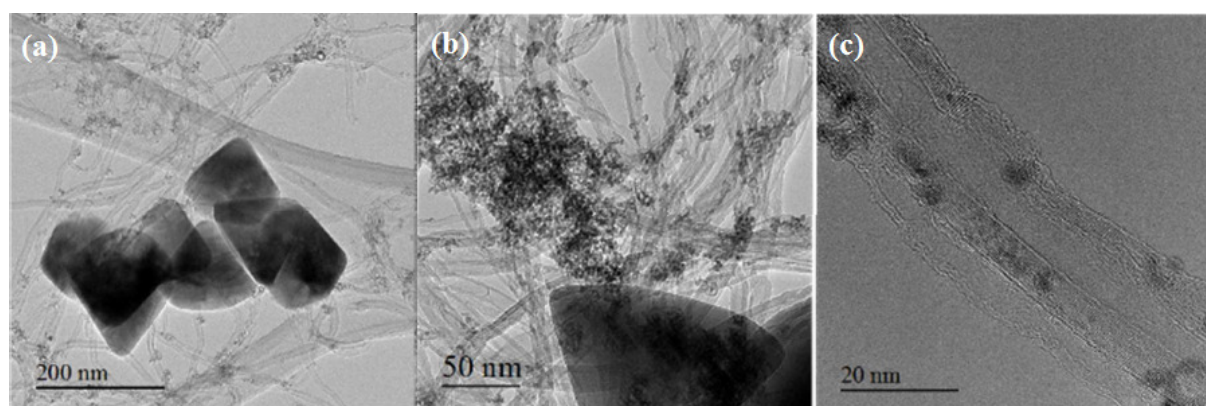


Figure 10. TEM images of HfO₂-CNTs (sonicated for 30 minutes) + ETCZn006 mixture sonicated for 30 minutes, (a) overview of the nanomaterial, (b) magnification of the structure, (c) high magnification of the nanohybrid material.

In Figure 10(a) we see that there are two different shapes of nanoparticles: triangular and hexagonal. The dimension of particles is around 120 to 170 nm. HfO₂ NPs are evenly distributed along the CNTs. In Fig. 10(b) it is clearly see that the HfO₂ and ZnO nanoparticles are attached to CNTs. Carbon nanotubes are about 7 to 10 nm in diameter. Higher magnification of the material Fig. 10(c) shows that HfO₂ NPs are attached to CNTs not only in the defects but also on the straight part with no topological defects as well.

5.1.3.2 NANO_{H2}

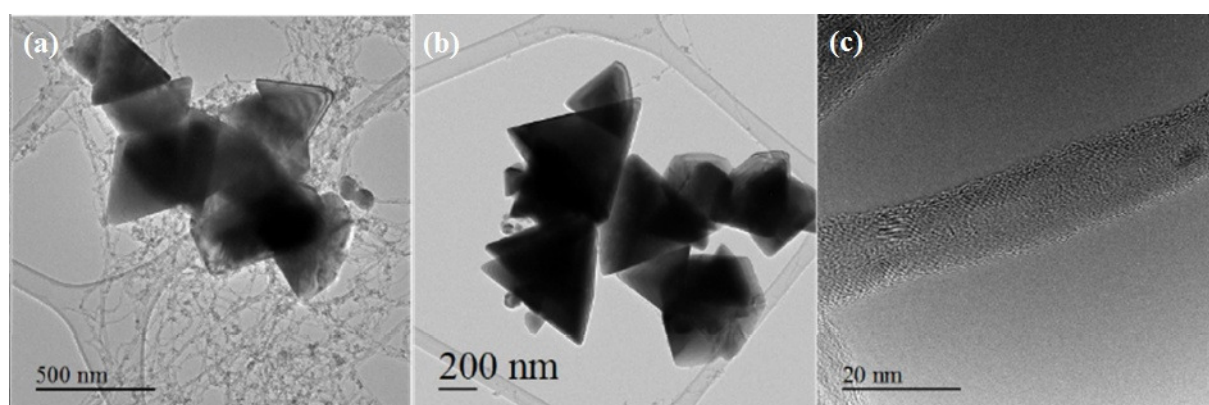


Figure 11. TEM images of HfO₂-CNTs (sonicated for 30 minutes) + ETCZn005 mixture sonicated for 5 minutes, (a) overview of the nanomaterial, (b) magnification of the structure, (c) high magnification of the nanohybrid material.

Comparing images Fig. 10(a) and Fig. 11(b) one clearly sees that NPs are sharper faceted on Fig. 11(b). The same is observed in Fig. 11(a). Figure 11(a) consists of triangular shaped NPs with diameters of 280 to 450 nm. There are also two smaller particles with 80 nm diameter and are round in shape. At least one ZnO particle is shaped like rhombus with length of one side 380 nm and the other 330 nm. HfO₂ and CNTs are remarkably smaller in dimensions. On the high magnification image of the sample Fig. 11(c) we can see that CNTs have diameter of 15 nm and HfO₂ particles are in the range of 2 to 3 nm [44]. In Fig. 11 b), one observes a variation of shape and size of nanoparticles. Width for the bigger triangular shaped NPs is around 650 nm and for the small hexagonal shaped around 50 to 90 nm.

5.1.3.3 NANO H_3

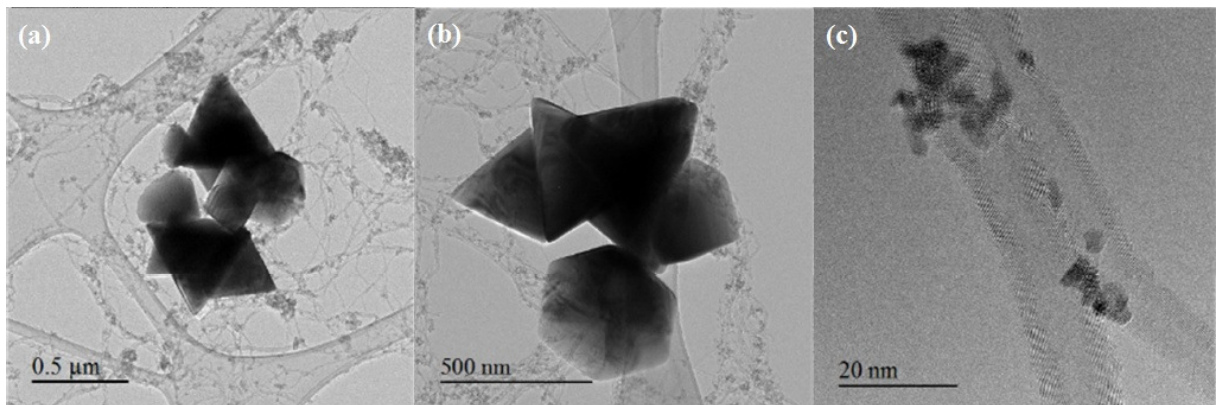


Figure 12. TEM images of HfO_2 -CNT-s (sonicated for 30 minutes) + ETCZn006 mixture sonicated for 90 minutes, (a) low magnification of the nanomaterial, (b) overview of the nanomaterial, (c) high magnification of the nanohybrid material.

The dimensions of NPs vary over a wide range. In Figure 12(a) 3 triangular shaped ZnO particles have sides of 530 nm. Other smaller particles (quadrilateral and hexagonal) have the diagonal width of around 370 nm. There is also ZnO particles with irregular shapes (dimensions around 200 to 300 nm). If we compare Fig. 11(a) and Fig. 12(b) then it is clear that Fig. 12(b) presents a better distribution of CNTs. In Fig. 12(b), it is noticeable that CNTs have a good contact with ZnO and HfO_2 nanoparticles. Figure 12(c) reveals that the HfO_2 nanoparticles are connected with CNTs and the connectivity is higher in the defective parts on CNT. The same result can be seen in Mr. M.Salumaa's last year's research on Figure 19(c) also on the Figures 20(b) and (c) [44].

5.1.3.4 NANO4

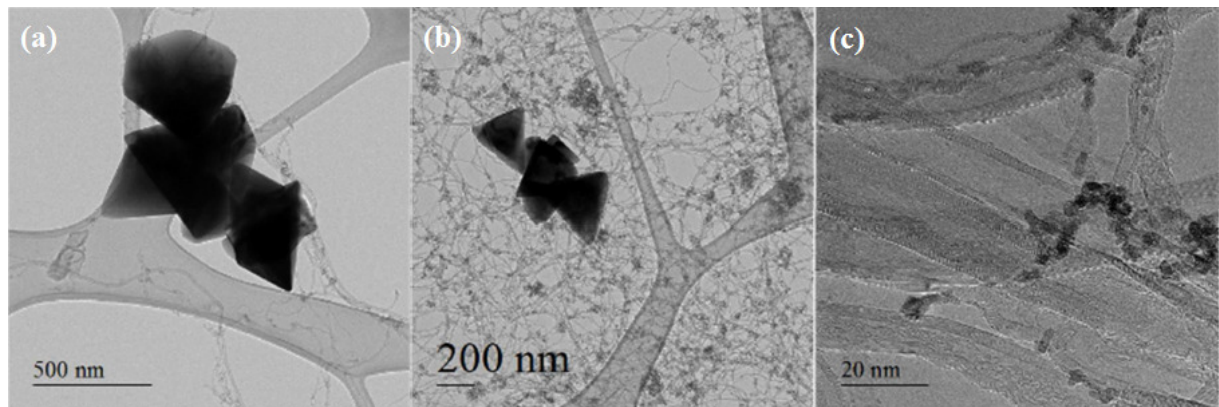


Figure 13. TEM images of HfO₂-CNTs (sonicated for 90 minutes) + ETCZn005 mixture sonicated for 5 minutes.

In Figure 13(a) one observes that the ZnO NPs are in contact with CNTs, also visible in Fig. 13(b). Size of the ZnO nanoparticles is in the range of 200–550 nm in diameter. The ZnO particles are located close to each other. The distribution of the CNTs as we see in Fig. 13(b) is very good. Also the HfO₂ NPs are quite evenly spread out. Higher magnification (c) shows that the CNTs have different diameter and the HfO₂ NPs are located not only on the defected parts but also on the sidewalls.

5.2 Electrical measurements

To determine the electrical properties of ZnO-HfO₂-MWCNTs nanohybrid material, I-V measurements were carried out. The IV-curves were linear for all the samples tested. The measurements to NANO1 to NANO4 samples showed that ZnO nanoparticles have isolating properties and this affects the electrical conductivity of the nanohybrid material. To confirm this hypothesis, IV-curves were measured on all the samples at least five different measuring points (for example NANO3 on Figure 14) and compared with the nanohybrid material (MS001) prepared by Martin Salumaa and tested same way (Fig. 16). This material served as a reference and it has been checked that it showed any degradation of its electrical properties after one year of shelf life. Samples were sonicated starting from zero minute sonification time to 180 minutes for the longest sonification treatment. From Martin Salumaa work, the optimized sonification duration is found to be around 30 min. To investigate even further the effect of sonification duration, new samples were synthesized: 10, 20 and 40 minutes sonification time samples were prepared and tested for electrical conductivity.

The photocurrent measurements were first done by illuminating the samples with a halogen lamp and at the same time measuring voltage dependent current to see if optical excitation had any effect on the electrical properties. It was expected that light would excite the nanoparticles and cause charge generation on the surface of the nanoparticles due to the surface states. ZnO and HfO₂ nanoparticles are luminescent in pure form; here these 2 types of nanoparticles were combined with CNTs. However, the luminescent effect of ZnO nanoparticles was not present. Samples were also tested under UV light which also showed no difference in conductivity. This was repeated with all the samples containing ZnO nanoparticles that were prepared on different temperature supports. In order to see if photo-generation occurs in these samples, short-circuit current was recorded with time but no additional current was observed under illumination compared to dark residual current.

Then the study was focussed on HfO₂NP-CNT nanocomposite. First, the electrical conduction was measured as a function of sonification duration from 10 to 40min. 30 minutes seems still to be the optimized sonification time. No significant difference on the conductivity was observed when the t=30min sample is placed on a heated and on a room temperature support (Fig. 16 and 17), even if a larger dispersion is noted for the heated support

Second step was to control the photocurrent properties on the sample MS001 (t=30 min) respectively deposited on room temperature support (Figure 15) and heated support (Figure 18 and 19). The current under 0V bias is recorded with time, the variations of the current were observed each time the light is switched on and off.

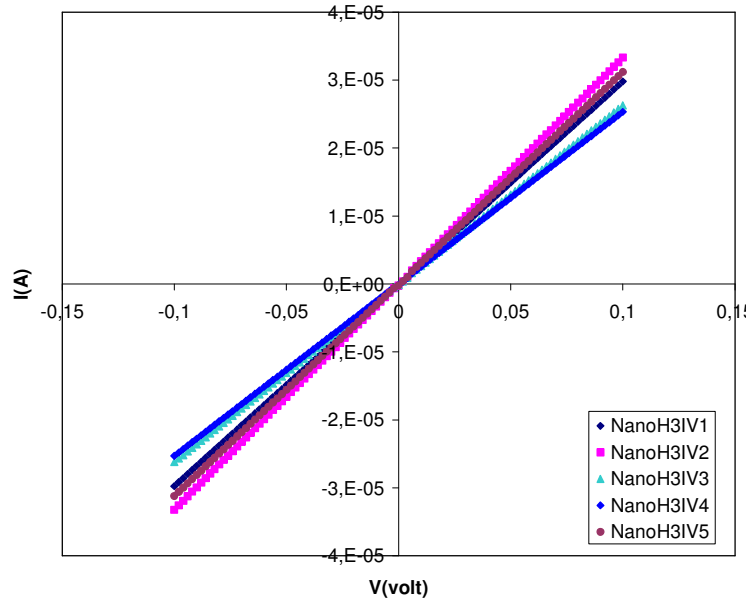


Figure 14. IV curve of the sample NANO3H for measuring electrical conductivity.

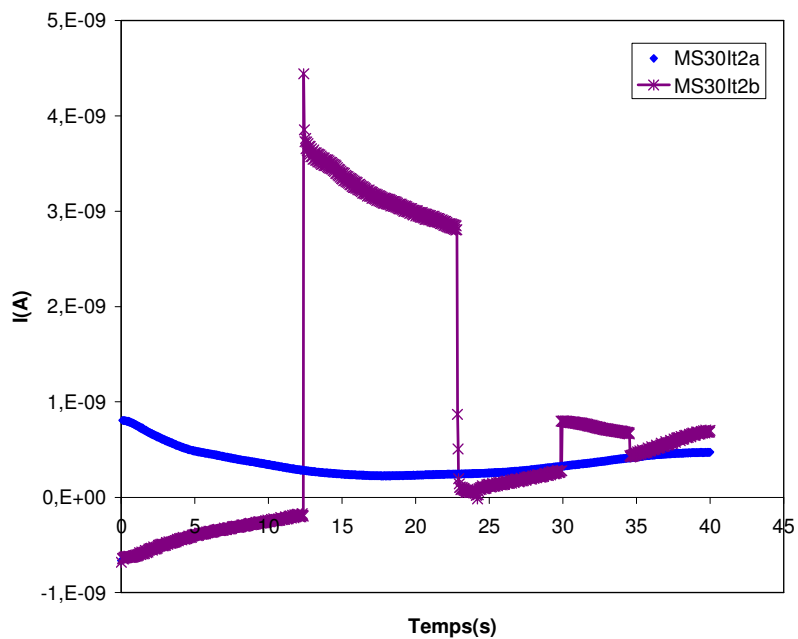


Figure 15. Current vs time under a polarization of zero volts. Most promising sample MS001 (t=30min) on room temperature support. 2a measurement corresponds to measure of reference on the sample where no effect photocurrent could be detected. 2b shows the material region where photocurrent effect appeared due to the presence of large amounts of nanoparticles.

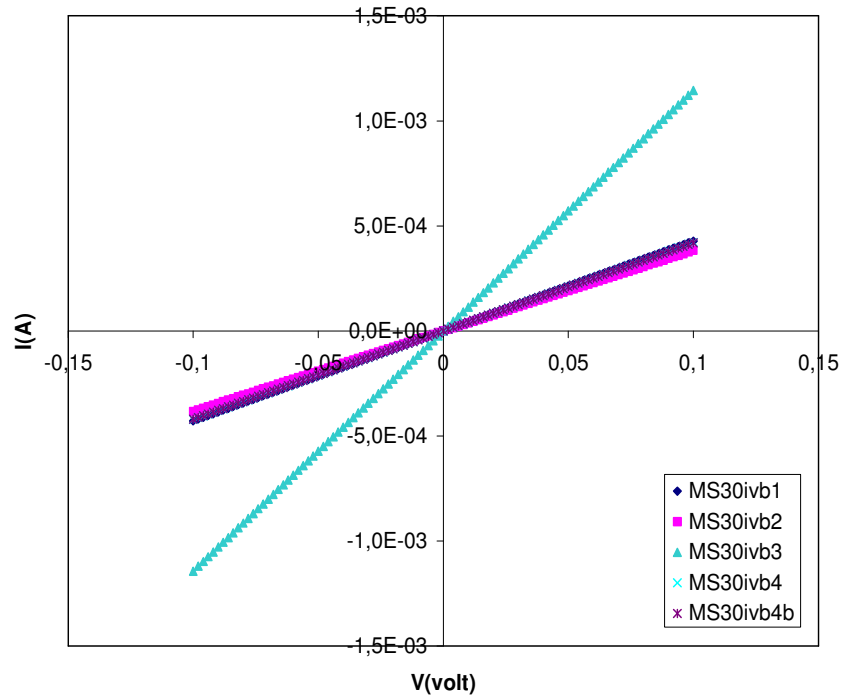


Figure 16. IV curve of sample MS001 ($t=30$ min) on room temperature support for measuring the electrical conductivity properties.

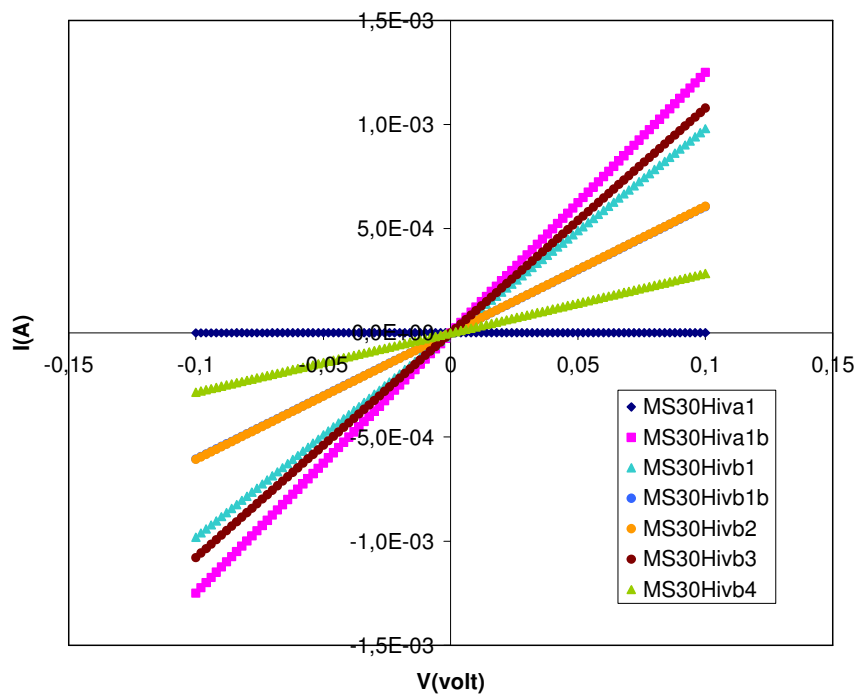


Figure 17. IV curve of sample MS001 ($t=30$ min) on heated support for measuring the electrical conductivity properties.

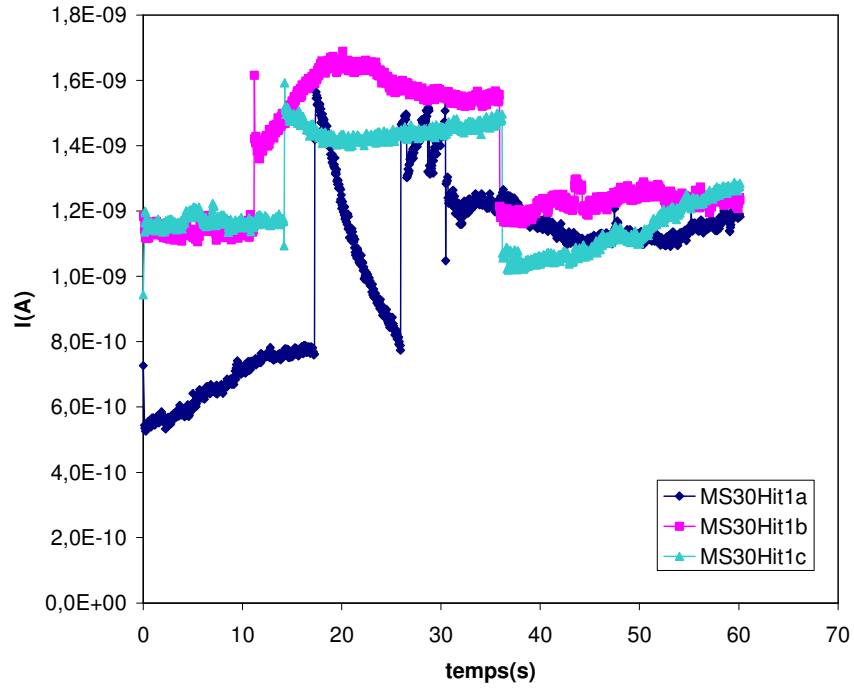


Figure 18. Current vs time under a polarization of zero volts. Sample MS001 ($t=30\text{min}$) on heated support. 3 measurements showed response to both visible light and UV.

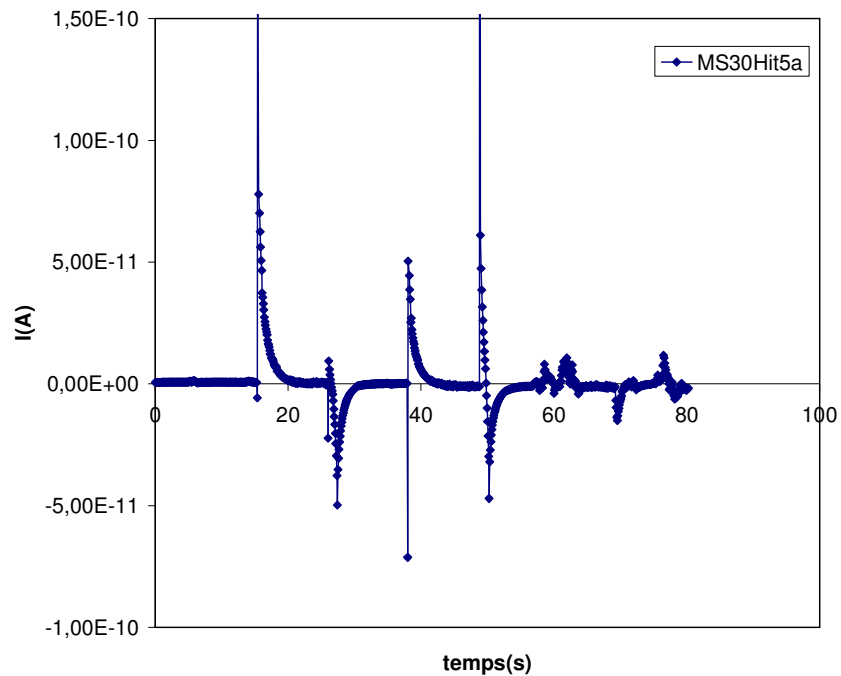


Figure 19. Current vs time under a polarization of zero volts. Sample MS001 ($t=30\text{min}$) on heated support. Sample corresponded to the visible light switching.

6. DISCUSSION

6.1 TEM studies of ZnO NPs, MWCNT–ZnO NPs

Zinc oxide NPs were synthesized via non-aqueous sol-gel process at different temperatures. This method is used to synthesize very pure and highly crystalline ZnO NPs. In this research work, it was synthesized zinc oxide NPs at 200, 240 and 300°C. The next step was to synthesize hybrid nanocomposite combining carbon nanotubes and zinc oxide. The TEM study highlighted that the ZnO NPs synthesized without CNT (ETCZn006) have a larger diameter (50-400 nm) than the ZnO nanoparticles synthesized in the presence of CNTs (ETCZn005, diameter of 50 to 100 nm). Based on this, it can be said that CNTs may affect the ZnO nanoparticles growth during the synthesis process.

6.2 TEM studies of MWCNT – ZnO – HfO₂, effects of sonication

The aim of this thesis was to confirm and improve the results obtained by Mr. M. Salumaa during his study on nanohybrid material combining HfO₂ nanoparticles and CNTs. For that it has been added to MWCNT-HfO₂ nanohybrid some ZnO NPs in pure form or mixed with CNTs. Samples NANO1 and NANO3 were prepared with pure ZnO NPs and NANO2 and NANO4 prepared using ZnO NPs synthesized with CNTs (Table 2). The comparison of Fig. 10 and Fig. 11 shows a higher concentration of CNTs in NANO2. Similar result is visible via the comparison of Figure 12 and 13. Finally, ZnO NPs edges seem to be sharper with the increase of temperature synthesis.

6.3 Electrical measurements

Almost 170 electrical measurements were performed on MWCNT-ZnO-HfO₂ and MWCNT-HfO₂ hybrid nanocomposites. Unfortunately, ZnO based nanohybrids did not give the expected results. All the samples, including free-standing ZnO NPs have shown low electrical conductivity and did not show any electrical response under UV or visible light excitation. Although under UV lamp excitation the samples (NANO1 to NANO4) exhibited luminescent responses, no photocurrent response was observed.

This study showed that the addition of ZnO nanoparticles to HfO₂ carbon based nanohybrid does not enhance the photocurrent properties. The previous investigation performed by Mr.

M. Salumaa has shown that a high concentration of HfO₂ NPs on CNTs is necessary to observe a photocurrent response under UV excitation. In our case, the first experiments showed that HfO₂ nanoparticles concentration was too low compared to the CNT content. In addition, instead of using UV lamp, the utilization of a laser would be more effective for such study.

The electrical measurements were performed on all the samples to get as much information as possible and compare the data. Electrical properties studies were then performed on CNT-HfO₂ samples with sonication time of 0 minute, 10 minutes, 20 minute, 30 minutes, 40 minutes, 120 minutes, 180 minutes and with a good dispersion of CNTs and NPs on the surface of the glass substrate. For better preparation of the sample it was decided to heat the glass substrate to speed-up the ethanol evaporation. The measurements on samples MS001 (sonication duration of 30min) have demonstrated similar response under light excitation on both heated and room temperature substrates. Figures 15 and 18 show the photocurrent response of the samples under light and UV excitation. Even though the measured currents were only around 1-3 nA, it confirms the photocurrent properties of these hybrid nanocomposites. After several attempts, it was managed to record on sample MS001 (t=30, on heated support) a capacitive response under UV light. In both samples we have observed that this area contained a higher concentration of HfO₂ nanoparticles compared to CNTs amount. The electrical conductivity was also measured in this area (Fig. 17). This area exhibited bluish-green luminescence that is characteristic of HfO₂ nanoparticles. Compared to ZnO based samples the electrical conductivity is more than ten times higher (sample MS001 t=30min electrical conductivity is about 13 times better than NANO H₃). With these measurements, we confirm the results of Mr Salumaa concerning the effect of illumination on the current of MS001 sample with an optimized time sonification of 30min. However, contrary to the best results that he obtained, showing the generation of stable photocurrent on a part of the sample with a high concentration HfO₂ nanoparticles so called "hafnium clusters", our photoresponse is not stable and does not contribute to a continuous photogenerated current under illumination. This shows that the transport of the photogenerated charges remains a key point to be optimized.

7. SUMMARY AND CONCLUSION

The main objective of this Masters' thesis was to conduct a research on new hybrid nanocomposites combining carbon nanotubes) with metal oxide nanoparticles and more particularly on CNT-ZnO-HfO₂ and CNT-HfO₂. For that purpose, pure ZnO nanoparticles and ZnO mixed with CNT were synthesised via non-aqueous sol-gel method. These nanoparticles were then mixed with CNT-HfO₂ nanohybrid material already available using sonication methods. Also this study focused on the effects of the ultrasound on the CNT and how the ultrasounds affect ZnO, HfO₂ nanoparticles bonding on CNTs surface. Ultrasound treatment was used to disperse the CNTs and promote the anchoring of ZnO and HfO₂ nanoparticles on the surface of the CNTs. The electrical properties and photoconductivity of both hybrid nanocomposites were investigated via collaboration with Minatec in Grenoble, France. The ZnO nanoparticles used in this study were synthesized by Mr. Andres Aasna under the supervision of Prof. Erwan Rauwel. Hafnium based nanohybrid used for this thesis were prepared by Mr. Martin Salumaa under the supervision of Prof. Erwan Rauwel.

The first part of this thesis was to prepare a new mixture of ZnO and CNTs. The purpose of this was to study how CNTs affect ZnO nanoparticles synthesis results. Also to see how the temperature change affects the nanoparticles size and shape. The second part was to use ultrasound treatment for the preparation of ZnO-HfO₂-CNT hybrid nanocomposites. Former mixture of 6 mg of MWCNTs mixed with 7.9 mg of HfO₂ cubic nanoparticles from sample ERHfO001 were mixed with 4.8 mg of ZnO nanoparticles. Similar process was used for the preparation of ZnO-CNT hybrid nanocomposite. For this Masters' thesis ten samples have been synthesized or prepared.

The HRTEM study was carried out under the supervision of Dr. Protima Rauwel who performed the HRTEM study. The goal of this study was to understand the effect of sonication duration on the dispersion of the hybrid nanocomposite and the anchoring of the metal oxide nanoparticles (ZnO and HfO₂) on the surface of the carbon nanotubes. This study has confirmed that ultrasound treatment affects the dispersion of the materials in the solution and has further helped us to understand how the nanoparticles attach on the surface of the non-functionalized CNTs. The sonication treatment results were similar to the ones obtained by Mr. M. Salumaa. Sonication duration time improves the anchoring of NPs and creates or modifies the defects in the structure and on the surface of the CNTs.

The electrical measurements were carried out to confirm the photocurrent generation observed by Mr. Martin Salumaa on HfO₂-MWCNTs hybrid nanocomposites. The second objective was to study the photoelectrical properties of ZnO-HfO₂-CNT hybrid nanocomposites and compare these properties to the former nanocomposites. We have observed that electrical conductivity of the HfO₂-CNT hybridnanocomposites is considerably superior to the samples containing ZnO nanoparticles. This study showed that the addition of ZnO nanoparticles to HfO₂-CNT hybrid nanocomposites does not seem to improve the properties. It could also be due to a lower amount of HfO₂ nanoparticles in these samples and the fact that ZnO nanoparticles do not behave like HfO₂ nanoparticles under UV excitation. The higher energy source like a laser would be more suitable for this study. Future investigation will then involve the utilization of laser instead of UV lamp in the case of ZnO nanoparticles. This study has also demonstrated that more investigations on these hafnium-carbon nanohybrid materials need to be performed to fully understand the mechanism that produces photocurrent under UV or light excitation. More particularly the influence of the ratio HfO₂ NPs/CNTS has to be studied in detailed. Such study will be possible with the future acquisition of a glove box by Tartu College.

In summary, this study confirmed the photoresponse observed by Mr. Martin Salumaa and has demonstrated the reproducibility of these results. These new HfO₂-CNT hybrid nanocomposites exhibit a photocurrent under UV or light excitation. It has been shown that the addition of ZnO nanoparticles to hybrid nanocomposites does not improve the photocurrent properties of the above mentioned material if a UV lamp is used as an excitation source. It has been demonstrated once again that ultrasonic treatment is an effective method for introducing functionalities to non-functionalized CNTs and anchoring MONP on their surface. Hafnium based nanohybrid appears to be a promising material for future energy harvesting applications. The complete understanding of HfO₂-CNT nanohybrid materials properties needs more investigation and will be the focus of future investigations.

ACKNOWLEDGEMENTS

First of all I would like to thank my supervisors Prof. Erwan Rauwel and Dr. Protima Rauwel for their professionalism, knowledge, guidance and support over the period of writing this thesis. This project was initiated by Dr. Protima Rauwel and its realization would not have been possible without both of my supervisors and I do not have enough words to express my gratitude towards them. Dr. Frédérique Ducroquet from MINATEC, Grenoble, France for all her help and guidance in electrical measurements carried out via the PARROT program exchange during my stay in Grenoble. I would like to thank all the staff at Tallinn University of Technology, Tartu College for supportive information and understanding. I also want to acknowledge all my friends, fellow students and family who provided me with all kind of support, especially my wife and daughter, parents.

REFERENCES

1. Official website of the United States National Nanotechnology Initiative, Nanotechnology Timeline. [WWW] <http://www.nano.gov/timeline> (28.01.2016).
2. M. Reibold, P. Paufler, A. A. Levin, W. Kochmann, N. Pätzke, D. C. Meyer, Materials: Carbon nanotubes in an ancient Damascus sabre- Nature 444, 286, 2006 [Online] Macmillan Publishers Limited (17.02.2016).
3. N. Taniguchi, "On the Basic Concept of 'Nano-Technology'", Proceedings of the International Conference on Production Engineering, Tokyo, 1974, Part II (Japan Society of Precision Engineering).
4. There's Plenty of Room at the Bottom. An Invitation to Enter a New Field of Physics. [WWW] <http://www.zyvex.com/nanotech/feynman.html> (11.02.2016).
5. E. K. Drexler, Engines of Creation. The Coming Era of Nanotechnology, 1986 [Online book] http://e-drexler.com/d/06/00/EOC/EOC_Table_of_Contents.html (17.02.2016).
6. IWGN Workshop Report, U.S. National Science and Technology Council, 1999, Washington D.C. [Online] <http://www.wtec.org/loyola/nano/IWGN.Research.-Directions/> (17.02.2016).
7. Official website of the Colleges of Nanoscale Science and Engineering. [WWW] <http://www.sunyense.com/AboutUs/History.aspx> (18.02.2016).
8. Estonian Nanotechnology Competence Centre official homepage. [WWW] <http://encc.ee/> (31.03.2016).
9. Online Browsing Platform of the International Organization for Standardization. [WWW] <https://www.iso.org/obp/ui/#iso:std:iso:ts:80004:-2:ed-1:v1:en> (18.02.2016).
10. M. M. Berekaa, Nanotechnology in Food Industry; Advances in Food processing, Packaging and Food Safety, International Journal of Current Microbiology Applied Sciences (2015) 4(5): 345-357.
11. T.V. Pfeiffer, J. Ortiz-Gonzalez, R. Santbergen, H. Tan, A. S. Ott, M. Zeman, A.H.M. Smets, Plasmonic nanoparticle films for solar cell applications fabricated by size-selective aerosol deposition, ScienceDirect, Energy Procedia 60 (2014) 3 – 12.
12. J. A. Rodriguez, M. Fernandez-Garcia, Synthesis, properties, and applications of oxide nanomaterials, Published by Wiley & Sons, Inc., Hoboken, New Jersey, 2007.
13. Official website of Ruchira Wijesena. [WWW] https://ninithi.com/topdown_methods/ (15.04.2016).

14. T. P. Yadav, R. M. Yadav, D. Pratap Singh, Mechanical Milling: a Top Down Approach for the Synthesis of Nanomaterials and Nanocomposites, *Nanoscience and Nanotechnology*, 2012. [Online] Scientific & Academic Publishing.
15. E. Matijević, W. P. Hsu, Preparation and properties of monodispersed colloidal particles of lanthanide compounds: I. Gadolinium, europium, terbium, samarium, and cerium(III), *Journal of Colloid and Interface Science*, August 1987, volume 118, issue 2, pp. 303-599.
16. T. Adschiri, Y. Hakuta, K. Sue, K. Arai, Hydrothermal Synthesis of Metal Oxide Nanoparticles at Supercritical Conditions, *Journal of Nanoparticle Research*, June 2001, volume 3, issue 2, pp. 227-235.
17. T. Adschiri, Y. Hakuta, K. Sue, K. Arai, Hydrothermal synthesis of metal oxide nanoparticles at supercritical conditions, *Journal of Nanoparticle Research*, Jun 2001, volume 3, issue 2, pp. 227-235.
18. T. Adschiri, Y. Hakuta, K. Sue, K. Arai, Hydrothermal synthesis of metal oxide fine particles at supercritical conditions, *Ind. Eng. Chem. Res.* 2000, volume 39, pp. 4901–4907.
19. T. Adschiri, Y. Hakuta, K. Sue, K. Arai, Hydrothermal synthesis of metal oxide nanoparticles at supercritical conditions, *J. Nanopart. Res.* 2000, volume 3, pp. 227–235.
20. Y. Hakuta, H. Hayashi, K. Arai, Fine particle formation using supercritical fluids, *Curr. Opin, Solid State Mater. Sci.* August–October 2003, volume 7, Issues 4 – 5, pp. 341–351.
21. M. Niederberger, Nonaqueous Sol–Gel Routes to Metal Oxide Nanoparticles, *Accounts of Chemical Research*, October 2007, volume 40, Issue 9, pp. 793–800.
22. M. Niederberger, N. Pinna, *Metal Oxide Nanoparticles in Organic Solvents, Synthesis, Formation, Assembly and Application*, 2009, volume 8, pp 12–15.
23. J. Ba, *Nonaqueous Syntheses of Metal Oxide Nanoparticles and Their Assembly into Mesoporous Materials*, PhD Dissertation, Potsdam, The Max Planck Institute of Colloids and Interfaces, June 2006.
24. C. Lind, S. D. Gates, N. M. Pedoussaut, T. I. Baiz, *Novel Materials through Non-Hydrolytic Sol-Gel Processing: Negative Thermal Expansion Oxides and Beyond*, *Materials* 2010, volume 3, pp. 2567-2587.
25. C.W. Bunn. A Comparative Review of ZnO Materials and Devices, *Proc. Phys.Soc.*, London, 47, 1935, 835.
26. U. Ozgur, Y.I. Alivov, C. Liu, A. Teke, M.A. Reshchikov, S. Dogan, V. Avrutin, S.J. Cho, H. Morkoc, A comprehensive review of ZnO materials and devices, *J Appl Phys*, 98(2005), 041301-041103.

27. K. Kim, B. Jung, J. Kim, W. Kim, Organic solar cells embedded with ZnO nanoparticles, 2009 [WWW] http://cap.ee.ic.ac.uk/~pdm97/powermems/2009/pdfs/papers/074_0194.pdf (30.04.2016)
28. P. K. Shrestha, Y. T. Chun, D. Chu, A high-resolution optically addressed spatial light modulator based on ZnO nanoparticles, *Science & Applications*, 2015, volume 4, pp. 259. [Online]
29. U. Philipose, G. Sapkota (2012). Ferromagnetic ZnO Nanowires for Spintronic Applications, *Nanowires - Recent Advances*, Prof. Xihong Peng (Ed.), InTech, DOI: 10.5772/52825. Available from: <http://www.intechopen.com/books/nanowires-recent-advances/ferromagnetic-zno-nanowires-for-spintronic-applications> (30.04.2016)
30. Z. Q. Zheng, J. D. Yao, B. Wang, G. W. Yang, Light-controlling, flexible and transparent ethanol gas sensor based on ZnO nanoparticles for wearable devices, *Scientific Reports* 5, 2015, article number: 11070. [Online]
31. R. Pati, R. K. Mehta, S. Mohanty, A. Padhi, M. Sengupta, B. Vaseeharan, C. Goswami, A. Sonawane, Topical application of zinc oxide nanoparticles reduces bacterial skin infection in mice and exhibits antibacterial activity by inducing oxidative stress response and cell membrane disintegration in macrophages, *Nanomedicine: Nanotechnology, Biology, and Medicine*, August 2014, volume 10, issue 6, pp. 1195–1208. [Online]
32. S. Geller, E. Corenzwit, Hafnium Oxide, HfO₂ (Monoclinic), *Analytical Chemistry*, 1953, volume 25, issue 11, pp. 1774–1774.
33. P. Rauwel, E. Rauwel, C. Persson, M. F. Sunding, A. Galeckas, One step synthesis of pure cubic and monoclinic HfO₂ nanoparticles: Correlating the structure to the electronic properties of the two polymorphs, *Journal Of Applied Physics*, 2012, 112, 104107-1.
34. P. R. Bandaru, *Electrical Properties and Applications of Carbon Nanotube Structures*, *Journal of Nanoscience and Nanotechnology*, 2007, volume 7, pp. 1–29. [Online] American Scientific Publishers
35. A. Szabó, C. Perri, A. Csató, G. Giordano, D. Vuono, J. B. Nagy, *Synthesis Methods of Carbon Nanotubes and Related Materials*, *Materials* 2010, volume 3, pp. 3092-3140.
36. J. I. Centre, Transmission electron microscopy (TEM). [WWW] https://www.jic.ac.uk/microscopy/intro_EM.html (22.02.2016).
37. P. Hirsch, *Electron microscopy of thin crystals*, London, Butterworths, 1965.
38. Prakash R. Somani, M. Umeno, Importance of Transmission Electron Microscopy for Carbon Nanomaterials Research, *FORMATX* 2007. [Onlyine]

39. D. B. Williams, C. B. Carter, Handbook of Nanophysics: The Transmission Electron Microscope, Transmission Electron Microscopy, Springer US, 2009, pp. 3-22.
40. Z. L. Wang, Zinc oxide nanostructures: growth, properties and applications. J. Phys.: Condens. Matter 16(2004) R829–R858.
41. F. J. Heiligt, M. Niederberger, The fascinating world of nanoparticle research, Materials Today, July/August 2013, volume 16, numbers 7/8.
42. Materials Characterization, X-ray Diffraction (XRD) Analysis. [WWW] <http://www.eag.com/mc/x-ray-diffraction.html> (10.05.2016)
43. Compare Transmission Electron Microscopes (TEMs) with Scanning Electron Microscopes (SEMs). [WWW] <http://www.ivyroses.com/Biology/Techniques/compare-TEM-vs-SEM.php> (15.05.2016)
44. M. Salumaa, Hybrid nanomaterials based on carbon nanodubes and metal oxide nanoparticles for photovoltaic applications: master thesis, Tartu, Tallinn University of Thecnology Tartu College, 2015.
45. E. E. Zainelabdin, Lighting and Sensing Applications of Nanostructured ZnO, CuO and Their Composites, Linköping Studies in Science and Technology, Dissertation, Norrköping, 2012, No. 1484. [Online]
46. W.H. Bragg, W.L. Bragg, "The Reflexion of X-rays by Crystals", Proc R. Soc. Lond, 1913, A 88 (605): 428–38.
47. N. Ahmad, Advanced Techinques for Materials Characterization lecture notes, [WWW] <https://materialsection.wordpress.com> (23.05.2016).
48. P. Scherrer, N. Göttinger, Gesell, 1918, 2, 98.
49. C. C. Koch, I. A. Ovid'ko, S. Seal, S. Veprek, Structural Nanocrystalline Materials: Fundamentals and Applications, Cambridge University Press, June 2007. [Online]
50. E. Rauwel, A. Galeckas, P. Rauwel, M. F. Sunding, H. Fjellvag, Precursor-Dependent Blue-Green Photoluminescence Emission of ZnO Nanoparticles, The Journal Of Physical Chemistry, 2011, 115, 25227-25233.